

GAMDTP: Dynamic Trajectory Prediction with Graph Attention Mamba Network

Yunxiang Liu¹, Hongkuo Niu¹, and Jianlin Zhu²

Shanghai Institute of Technology, Shanghai 10259, China
236142132@mail.sit.edu.cn

Abstract. Accurate motion prediction of traffic agents is crucial for the safety and stability of autonomous driving systems. In this paper, we introduce GAMDTP, a novel graph attention-based network tailored for dynamic trajectory prediction. Specifically, we fuse the result of self attention and mamba-ssm through a gate mechanism, leveraging the strengths of both to extract features more efficiently and accurately, in each graph convolution layer. GAMDTP encodes the high-definition map(HD map) data and the agents' historical trajectory coordinates and decodes the network's output to generate the final prediction results. Additionally, recent approaches predominantly focus on dynamically fusing historical forecast results and rely on two-stage frameworks including proposal and refinement. To further enhance the performance of the two-stage frameworks we also design a scoring mechanism to evaluate the prediction quality during the proposal and refinement processes. Experiments on the Argoverse dataset demonstrates that GAMDTP achieves state-of-the-art performance, achieving superior accuracy in dynamic trajectory prediction.

Keywords: Trajectory Prediction · Graph Attention Network · Mamba-ssm.

1 Introduction

Accurate motion forecasting of surrounding traffic agents, including vehicles, pedestrians, and other road participants, is critical to guarantee the safety and stability of autonomous driving systems. Predicting the trajectories of traffic agents with high precision allows autonomous systems to anticipate future states, make informed decisions in real-time and avoid risks while driving.

Researches in the early stage mainly used rasterized semantic images to represent map information[1,2]. However, due to the loss of information while rasterization, [3] and [4] both design a vector-based method that agents and roads are modeled as a collection of vectors. [5,6,7,8] are based on this and leverage GNNs[9] and LSTM[10] to fuse spatio-temporal information for accurate and socially plausible vehicle trajectory prediction. However, LSTM-based methods are bottlenecked by the parallelization, memory efficiency, long term dependencies and training speed. Recent advances in this domain such as HiVT[11], by considering the deep relationship between agents and scenario, agents and agents,

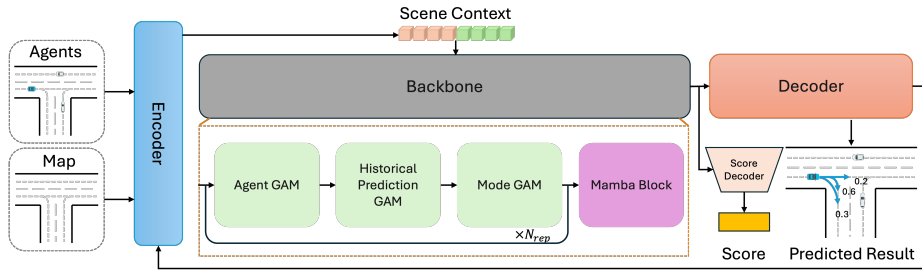


Fig. 1. Overview of GAMDTP. The encoder processes raw input features such as HD map and agent trajectory information. Our proposed Graph Attention Mamba module is applied in the components Agent GAM, Historical Prediction GAM and Mode GAM, which extracts spatio-temporal features. Decoder generates the final predicted trajectories and probability and the score decoder further evaluates and prioritizes trajectory candidates for refinement through generate a score for each result, ensuring accurate and reliable predictions.

as well as the selection of the direction of the coordinate system and other factors, the network achieves a fairly good effect. QCNet[12] further investigates the impact of reusing historical calculations on the final prediction results. They presents an efficient, multi-modal trajectory prediction framework using a novel tow-stage, consists of proposal and refinement, with query-centric paradigm. By reusing scene encodings and combining anchor-based refining strategies, it achieves both fast inference and high prediction accuracy, making it well-suited for real-time autonomous driving scenarios. Moreover, HPNet[13] integrates historical predictions with real-time context through its Historical Prediction Attention module, which dynamically models the relationship between successive predictions, resulting in more accurate and stable trajectory forecasts. In addition, many previous works[14,15,16,17,11,12,13] use multi-modal future trajectories as output rather than a single trajectory, given the uncertainty of future, and we also follow this way in this paper.

While most of those approaches are Graph Attention Networks (GAT)[9] based, which brings GNNs and Transformers together, and Transformers[18] can capture long range dependencies among nodes in a graph, they suffer from the limitation of quadratic computational complexity due to the self-attention mechanisms, making them less efficient for large-scale, real-time trajectory forecasting tasks. Recently, a brand new state space model (SSM)[19], Mamba[20,21], demonstrates potential in sequence modeling and long-term dependencies capturing with linear computational complexity and improved GPU efficiency across tasks in natural language processing[22,23,24] and computer vision[25,26,27]. Despite its potential, Mamba-SSM remains underexplored in the context of graph-based trajectory prediction frameworks.

To address these limitations, we propose GAMDTP, a novel module that fuses Graph Attention Networks (GAT)[9] with the selective capabilities of Mamba-

SSM[20]. Inspired by [28] in computational pathology, GAMDTP leverages the unique strengths of both GAT[9] and Mamba-SSM[21,20] through a gate mechanism, combining the self-attention mechanism’s adaptability to complex inter-agent interactions with Mamba’s efficient handling of long-range dependencies through structured state spaces. This fusion allows GAMDTP to deliver accuracy feature extraction efficiency, scalable computational performance, the ability to adapt to diverse and dynamic driving environments and making it particularly suited for real-time trajectory prediction.

Additionally, recognizing the limitations of existing two-stage trajectory prediction frameworks, where the proposal and refinement stages often lack effective cooperation, we introduce a Quality Scoring Mechanism following SmartRefine[29]. This mechanism evaluates the prediction quality at both stages, prioritizing high-quality trajectory proposals and improving the refinement process, ultimately leading to more accurate and reliable trajectory forecasts.

Our approach is evaluated on the Argoverse[30] and INTERACTION[31] datasets, both are standard benchmarks for autonomous driving scenarios, where GAMDTP demonstrates state-of-the-art performance. This enhancement in prediction capability not only strengthens the robustness of trajectory predictions but also contributes to the overall safety and stability of autonomous driving systems.

In summary, our work has the following contributions:

- We fuse GAT and Mamba as a novel graph neural network called GAM which combines Mamba module through a gate mechanism to dynamically balance local and global feature extraction.
- GAMDTP merges a score mechanism to evaluate the prediction results of proposal and refinement to improve the performance of the refine process.
- Experiments on the Argoverse[30] and INTERACTION[31] datasets demonstrate that GAMDTP achieves the state-of-the-art performance.

2 Related work

2.1 GNNs and Temporal Models for Trajectory Prediction

The development of accurate and efficient trajectory prediction models is critical for autonomous driving, as they allow for anticipating the future states of traffic agents ensuring safety and operational stability for real-time decisions. To model the social spatial and temporal interactions between agents and agents, agents and lanes, [4,5] apply message-passing GNNs and encode agents and lanes as nodes, speed, direction and other dynamic information as edges. GNNs work by iteratively gathering information from neighboring nodes to update the current node’s representation, with different GNN types employing distinct aggregation and update functions. This process enables GNNs to learn representations that encapsulate the graph data’s topological structure. To model history trajectory and other sequence data, early approaches relied heavily on Recurrent Neural Networks(RNNs)[32] and Long Short-Term Memory networks(LSTMs)[10] to

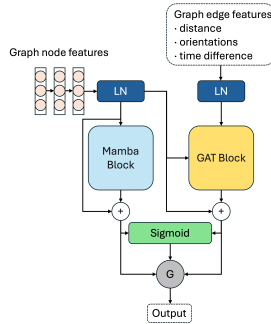


Fig. 2. Our proposed Graph Attention Mamba module, which integrates Mamaba block and graph attention block. The input features include node features and edge features, which first normalized through a Layernorm(LN) layer before processed by Mamba and GAT blocks. The output from these blocks are fused using a gate mechanism, where the sigmoid function dynamically generates a gate signal G to balance their contributions.

model temporal dependencies in sequential data[33,1]. LSTMs have been widely used in autonomous driving applications for their ability to maintain sequential information over time and handle agent-specific histories[34,35,36,8]. Compared to LSTMs, Transformers show more powerful in parallelization and long-term dependency capture, which impacts both training and memory efficiency. Therefore, attention mechanism[18] has become the dominant method adopted by recent[37,38]. [6,15,11,39,40] fuse GNNs and Transformers and model different scenarios toward different cases.

Recently, a novel state space model (SSM)[20], Mamba, has shown promise in sequence modeling and capturing long-term dependencies[19]. Mamba introduces a selective mechanism into the SSM, enabling it to identify critical information similarly to an attention mechanism. Studies have highlighted Mamba’s potential across domains like natural language processing[22,23,24] and computer vision. However, Mamba’s potential in combination with GATs remains underexplored. In this paper, we fuse Mamba and attention mechanism in graph neural network with a gate mechanism for encoding HD map data and historical trajectory information.

2.2 Two-Stage Motion Forecasting

Inspired by the refinement networks[41,42] in computer vision, refinement strategies have recently been applied in motion forecasting. This framework typically involves a proposal stage, where multiple candidate trajectories are generated, followed by a refinement stage, where these proposals are optimized based on the context. QCNet[12] employs a two-stage approach to improve efficiency and accuracy. Specifically, they leverages a query-centric paradigm to forecast the trajectory in the proposal stage and predict the offset in the refinement stage. HPNet[13] introduces a historical prediction attention module to encode the dy-

dynamic relation between successive predictions in the proposal stage and encodes the prediction with a two-layer MLP then recalculate the result in the same way in the refinement stage. But this does not produce better cooperation between the two stage. Inspired by SmartRefine[29], they introduce a brand new framework for refinement and design a quality score mechanism, we design a scoring mechanism between the proposal and refinement stage following HPNet[13].

3 Method

In this section, we first introduce problem formulation for dynamic trajectory prediction in 3.1. In order to verify the performance of the modules we designed and make our network easier to understand, we will introduce the selected backbone network in 3.2. Then, we present our proposed Graph Attention Mamba Network and the quality scoring mechanism in the two-stage framework in 3.3 and 3.4 respectively. Ultimately, we introduce the training objective with the loss function in 3.5.

3.1 Problem Formulation

The target of trajectory prediction is predicting the future paths of interested agents based on their past movements. Given a fixed-length sequence of history status frames, $\{f_{-T+1}, f_{-T+2}, \dots, f_0\}$, the goal is to predict K diverse possible trajectories for each of the N agents, as illustrated below:

$$L_0 = \{L_{0,n,k}\}_{n \in [1,N], k \in [1,K]} \quad (1)$$

where $f_t = \{a_t^{1 \sim N}, M\}$, $a_t^{1 \sim N}$ represents the features of all agents in the scene at time t , and M denotes the HD map including N_M lane segments. Specifically, $a_t^n = \{p_x^{t,n}, p_y^{t,n}, \theta^{t,n}, v_x^{t,n}, v_y^{t,n}, c_a^{t,n}\}$, where $(p_x^{t,n}, p_y^{t,n})$ means the location, $\theta^{t,n}$ is the orientation, $(v_x^{t,n}, v_y^{t,n})$ is the velocity and $c_a^{t,n}$ is the attribute. Every trajectory includes future locations for the next F time steps:

$$L_{0,n,k} = \{l_{1,n,k}, l_{2,n,k}, \dots, l_{F,n,k}\} \quad (2)$$

where $l_{i,n,k} \in \mathbb{R}^2$ represents the predicted position at time step i of mode k for agent n .

3.2 HPNet Backbone

Our work is based on a SOTA approach HPNet[13]. The encoder is applied by a two-layer MLP, following them, to encode the features of agents and HD map as embeddings:

$$E_a^{t,n} = MLP(v^{t,n}, \varphi^{t,n}, c_a^{t,n}) \quad (3)$$

$$E_m = MLP(l_m, c_m) \quad (4)$$

where $\varphi^{t,n}$ is the direction of velocity, l_m is the length of lane segments, c_m is the attributes of lane segments, $E_a^{t,n} \in \mathbb{R}^D$, $E_m \in \mathbb{R}^{M \times D}$, and D is the hidden dimension. Each agent at each time step and lane segment are treated as node in the graph. The edge features are represented as $\{d_e, \phi_e, \psi_e, \delta_e\}$, where d_e denotes the distance between the source and target nodes, ϕ_e represents the orientation of the edge in the reference frame of the target node, ψ_e is the relative orientation between source and target nodes, and δ_e corresponds to the time difference between them. The edge features are encoded into edge embeddings through a two-layer MLP $E_e = MLP(d_e, \phi_e, \psi_e, \delta_e)$, where $E_e \in \mathbb{R}^{Y \times D}$, Y is the number of edges. The output embeddings from the encoder as the input of Backbone, which contains three main modules driven by our proposed module namely Agent GAM, Historical Prediction GAM and Mode GAM respectively. Agent GAM first input the prediction embeddings $P_{t,n,k} = HP(E_m, E_e, E_a^{t,n})$, where function HP means the process method in HPNet[13], to model the interactions among agents. Then Historical Prediction GAM inputs the result of Agent GAM to model the correlation between historical predictions and current forecast. Finally, results of previous modules are entered into Mode GAM that models interactions among different future trajectory mode and the modules above are repeated $N_{rep} = 2$ times. To further model the sequence relationships, a Mamba block is employed at the end of the three modules.

3.3 Graph Attention Mamba Module with Gate Mechanism

An overview of our method is showed in Fig. 1. Our proposed module is applied in the Backbone and it is designed to enhance the feature extraction and prediction capabilities of the network. Specifically, as illustrate in Fig. 2, we use a Mamba2 layer as the Mamba block, graph attention network as GAT block, and the input graph node features and edge features are $P_{t,n,k}$ and $[P_{t,n',k}, E_e]$ respectively, where n' represents all agents within a radius of the n -th agent in the same time step and mode. Node features are passed into both Mamba block and GAT block, edge features are just pass through GAT block:

$$P_{t,n,k}^M = P_{t,n,k} + Mam(LN(P_{t,n,k})) \quad (5)$$

$$P_{t,n,k}^A = P_{t,n,k} + GAT(LN(P_{t,n,k}), LN(E_e)) \quad (6)$$

where function $Mam(a)$ represents the Mamba2 layer, a is the input sequence, GAT function is the graph attention layer, LN means layer normalization and $P_{t,n,k}^M$, $P_{t,n,k}^A$ is the output from the mamba block and GAT block.

We also design a gate mechanism to fuse $P_{t,n,k}^M$ and $P_{t,n,k}^A$:

$$G_{t,n,k} = \sigma(F_{fc}(P_{t,n,k}^M + P_{t,n,k}^A)) \quad (7)$$

$$P_{t,n,k}^G = P_{t,n,k} + G_{t,n,k} \cdot P_{t,n,k}^A + (1 - G_{t,n,k}) \cdot P_{t,n,k}^M \quad (8)$$

where $F_{fc}(X)$ is a fully connected layer, \cdot is the sigmoid function, $P_{t,n,k}^G$ is the output of the whole module.

3.4 Quality Scoring Mechanism

To enhance the performance of two-stage trajectory prediction framework, we introduce a scoring mechanism that evaluates the prediction quality of both the proposal and refinement stages. At the training stage, the quality of predicted trajectory can be assessed according to the ground truth trajectory and the predicted trajectory, inspired by SmartRefine[29]. In detail, using the maximum predicted error between the predicted result and the ground truth, represented by d_{max} , calculate the ratio of the absolute value of the difference between the proposal stage and refinement stage result and the absolute value of the difference between the refinement stage result and d_{max} to obtain the quality score:

$$q_{t,n} = \frac{|d_p - d_r|}{|d_{max} - d_r| + \epsilon} \quad (9)$$

where d_p is the predict error at proposal stage, d_r is the predict error at refinement stage. In order to ensure that the calculation is differentiable, we add a very small value ϵ that is not 0 to the denominator. To enable GAMDTP to predict the quality score, we utilize a Mamba2 layer to process the prediction embedding at proposal stage. Subsequently, an MLP is employed to produce the quality score, as show in Algorithm 1.

Algorithm 1 Scoring Mechanism in Training Stage

Input: Proposal section $f_{propose}$, refinement section f_{refine} , quality score decoder f_q , prediction error function f_e , score function Q , prediction error function Dis agent embeddings E_a , HD map embeddings E_m , edge embeddings E_e , ground truth trajectory p_{gt} , predict agent number N

Output: predicted score q_p , calculated score q

```

1:  $d_p, d_r, q, q_p$  []
2: for  $t = -T + 1, -T + 2, \dots, 0$  do
3:   for  $n = 1, 2, \dots, N$  do
4:     if  $n == 1$  ord  $disNone$  then
5:        $d_{max} = 0$ 
6:     end if
7:      $p = f_{propose}(E_a, E_m, E_e)$  {% proposal trajectory  $p$ }
8:      $q_p$  add  $f_q(p)$  {% trajectory refinement  $\Delta p$ }
9:      $\Delta p = f_{refine}(p, E_a, E_m, E_e)$ 
10:     $p_{out} = p + \Delta p$ 
11:     $d_p$  add  $Dis(p, p_{gt})$  {% propose prediction error  $d_p$ }
12:     $d_r$  add  $Dis(p_{out}, p_{gt})$  {% refine prediction error  $d_r$ }
13:     $d_{max} = \max(d_r, d_{max})$ 
14:     $q$  add  $Q(d_{max}, d_p, d_r)$ 
15:   end for
16: end for
17: return  $q_p, q$ 

```

Table 1. Comparison of GAMDTP with the state of the art methods on the Argoverse test set. The b-minFDE is the official ranking metric. For each metric, the best result is in **bold**, the second best result is underlined.

Method	b-minFDE ₆ ↓	minFDE ₆ ↓	minADE ₆ ↓	MR ₆ ↓	minFDE ₁ ↓	minADE ₁ ↓	MR ₁ ↓
LaneGCN[4]	2.0539	1.3622	0.8703	0.1620	3.7624	1.7019	0.5877
mmTransformer[40]	2.0328	1.3383	0.8436	0.1540	4.0033	1.7737	0.6178
THOMAS[43]	1.9736	1.4388	0.9423	<u>0.1038</u>	<u>3.5930</u>	1.6686	0.5613
HOME+GOHOME[44]	1.8601	1.2919	0.8904	0.0846	3.6810	1.6986	0.5723
DenseTNT[43]	1.9759	1.2815	0.8817	0.1258	3.6321	1.6791	0.5843
MultiModalTransformer[45]	1.9393	1.2905	0.8372	0.1429	3.9007	1.7350	0.6023
HiVT[11]	1.8422	1.1693	0.7735	0.1267	3.5328	1.5984	0.5473
Mutipath++[17]	1.7932	1.2144	0.7897	0.1324	3.6141	<u>1.6235</u>	0.5645
HPNet(w/o ensemble)[13]	1.7375	1.0986	<u>0.7612</u>	0.1067	3.7632	1.7346	0.5514
GAMDTP(ours)	<u>1.7690</u>	<u>1.1256</u>	0.7603	0.1088	3.8807	1.7813	<u>0.5509</u>

3.5 Training Loss

To optimize the proposed model, we follow the winner-takes-all strategy, which ensures that the most relevant mode, based on the minimum endpoint displacement, is selected for optimization. Specifically, the $k_{t,n}$ -th mode to be optimized is determined by minimizing the endpoint displacement between the predicted trajectory $\{L_{t,n,k}\}, k \in [1, K]$ and the ground truth trajectory $P_{t,n}^{gt} = \{P_{t+1,n}^{gt}, P_{t+2,n}^{gt}, \dots, P_{t+F,n}^{gt}\}$:

$$k_{t,n} = \arg \min_{k \in [1, K]} (l_{t+F,n,k}, P_{t+F,n}^{gt}) \quad (10)$$

Then two Huber losses are employed to optimize the trajectories both in proposal and refinement stage:

$$\mathcal{L}_{reg1}^{t,n} = \mathcal{L}_{Huber}(L_{t,n,k_{t,n}}^p, P_{t,n}^{gt}) \quad (11)$$

$$\mathcal{L}_{reg2}^{t,n} = \mathcal{L}_{Huber}(L_{t,n,k_{t,n}}^r, P_{t,n}^{gt}) \quad (12)$$

where $L_{t,n,k_{t,n}}^p$ is the predicted result in proposal stage, $L_{t,n,k_{t,n}}^r$ is in refinement stage.

The probability $\alpha_{t,n,k}$ for each predicted trajectory are optimized using a cross-entropy loss:

$$\mathcal{L}_{cls}^{t,n} = \mathcal{L}_{CE}(\{\alpha_{t,n,k}\}_{k \in [1, K]}, k_{t,n}) \quad (13)$$

For the quality scoring mechanism, we calculate the ℓ_1 loss between the predicted score $\hat{q}_{t,n}$ and labeled score $q_{t,n}$:

$$\mathcal{L}_s = \|\hat{q}_{t,n} - q_{t,n}\|_1 \quad (14)$$

In summary, final training objective combines the loss functions above:

$$\mathcal{L} = \frac{1}{TN} \sum_{t=-T+1}^0 \sum_{n=1}^N (\mathcal{L}_{reg1}^{t,n} + \mathcal{L}_{reg2}^{t,n} + \mathcal{L}_{cls}^{t,n} + \lambda \cdot \mathcal{L}_s) \quad (15)$$

Table 2. Comparison of GAMDTP with the state of the art methods on the INTERACTION test set. For each metric, the best result is in **bold**, the second best result is underlined.

<i>Method</i>	<i>minJointADE</i> ↓	<i>minJointFDE</i> ↓	<i>CCR</i> ↓
THOMAS[43]	0.4164	0.9679	0.1791
DenseTNT[15]	0.4195	1.1288	0.2240
Traj-MAE[46]	0.3066	0.9660	0.1831
HDGT[47]	0.3030	0.9580	0.1938
FJMP[48]	0.2752	0.9218	0.1853
HPNet(w/o ensemble)[13]	<u>0.2548</u>	0.8231	<u>0.1480</u>
GAMDTP(ours)	0.2529	<u>0.8295</u>	0.1474

where λ is a hyper-parameter to balance the four loss terms.

4 Experiments

4.1 Datasets

To evaluate the performance of our model, we conduct experiments on the Argoverse and INTERACTION datasets.

Argoverse[30] is a widely used benchmark for motion forecasting and perception tasks in autonomous driving. It comprises 324,557 interesting vehicle trajectories extracted from over 1,000 driving hours in real-world scenarios. This rich dataset includes high-definition (HD) maps and recordings of sensor data, referred to as “log segments,” collected in two U.S. cities: Miami and Pittsburgh. These cities were chosen for their distinct urban driving challenges, including unique road geometries, local driving habits, and a variety of traffic conditions.

INTERACTION[31] is a comprehensive resource designed to support research in autonomous driving, particularly in behavior-related areas such as motion prediction, behavior cloning, and behavior analysis. It offers a large-scale collection of naturalistic motions from various traffic participants, including vehicles and pedestrians, across a diverse set of highly interactive driving scenarios from different countries.

4.2 Metrics

We utilized standard trajectory forecasting metrics, ensuring a comprehensive assessment across different prediction scenarios. These metrics include evaluations on both Argoverse[30] and INTERACTION[31] datasets, capturing the accuracy, reliability, and multimodal capabilities of the predictions. For the Argoverse dataset, we employ minimum Average Displacement Error(minADE) and minimum Final Displacement Error(minFDE) to measure the accuracy of trajectory predictions. Specifically, minADE computes the average ℓ_2 -norm distance between the predicted trajectory and the ground truth across all time steps, while minFDE focuses on the ℓ_2 -norm distance at the final trajectory point.

Table 3. Ablation study on INTERACTION test set.

Backbone	Gate	Score	1-layer	3-layers	5-layers	minJointADE ↓	minJointFDE ↓	CCR ↓	minJointMR ↓
✓				✓		0.2641	0.8610	0.1515	0.1717
✓	✓			✓		<u>0.2543</u>	<u>0.8342</u>	<u>0.1473</u>	<u>0.1530</u>
✓		✓	✓			0.2641	0.8614	0.1516	0.1700
✓	✓	✓	✓			0.2529	0.8295	0.1474	0.1525
✓	✓	✓			✓	0.2643	0.8614	0.1511	0.1722
✓	✓	✓			✓	0.2706	0.8687	0.1548	0.1665

To further assess reliability, we included the Miss Rate(MR), which calculates the proportion of predicted trajectories whose endpoints deviate more than 2.0 meters from the actual ground truth endpoint. Additionally, we employed Brier Minimum Final Displacement Error(b-minFDE), which extends minFDE by integrating a confidence term $(1 - \hat{\alpha})^2$, where $\hat{\alpha}$ represents the predicted probability of the best trajectory. This metric combines endpoint accuracy with the model’s confidence, offering deeper insights into the reliability of its predictions. For the INTERACTION[31] dataset, we employ minJointADE, minJointFDE and Cross Collision Rate to evaluate the performance of joint trajectory prediction. Min-JointADE measures the average ℓ_2 -norm distance between the predicted and ground-truth trajectories of all agents, while minJoint FDE evaluates the ℓ_2 -norm distance at the final time step for all agents. To assess the model’s ability to capture multimodal outputs, we set $K = 6$ for both marginal and joint predictions.

4.3 Comparison with State-of-the-art

Results on Argoverse. The results for marginal trajectory prediction on the Argoverse[30] dataset are presented in Table 1. Our GAMDTP achieves the SOTA performance across all evaluation metrics among single models. Compared to HPNet[13], the second-best model on Argoverse leaderboard, GAMDTP improves from 0.7612 to 0.7603 in minADE where mode number $K = 6$ and from 0.5514 to 0.5509 in MR where mode number $K = 1$. These improvements highlight the effectiveness of our model in accurately capturing both trajectory endpoints and multimodal predictions. We show some examples in Fig. 3.

Results on INTERACTION. Table 2 presents the performance of our method on the INTERACTION[31] multi-agent track, where we achieved state-of-the-art results. Our approach outperformed the first-ranked FJMP[48] by a significant margin, with improvements of 0.0223 in minJointADE, 0.0923 in min-JointFDE and 0.0379 in Cross Collision Rate(CCR). Improve about 4% in CCR and 0.0019 in minJointADE compared to backbone HPNet[13]. These results demonstrate that our GAMDTP is both a simple and effective solution for joint trajectory prediction.

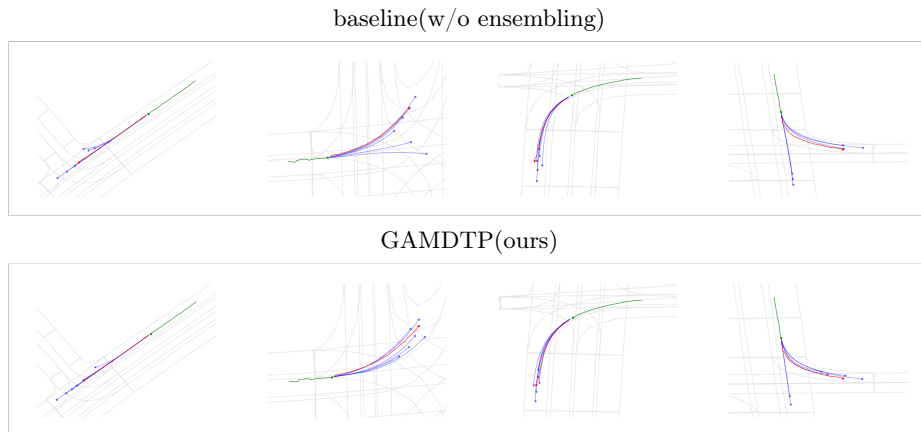


Fig. 3. Comparison our GAMDTP with baseline.

4.4 Ablation Study

To check the effectiveness of the key components in our model, we conduct a series of ablation experiments on the INTERACTION[31] test set. Specifically, we evaluate the impact of the gate mechanism, quality scoring mechanism and the number of Mamba layers. The results are summarized in Table 3.

Effect of gate mechanism. The gate mechanism in our GAMDTP module dynamically balances the contributions of the GAT and Mamba-SSM outputs. To analyze its effectiveness, we compare the model’s performance with and without the gate mechanism. As shown in Table 3, the removal of the gate mechanism leads to a noticeable drop in performance, increase minJointADE from 0.2529 to 0.2641, minJointFDE from 0.8295 to 0.8614 and the Cross Collision Rate(CCR) from 0.1474 to 0.1516. These results highlight the importance of dynamically balancing the contributions of GAT and Mamba-SSM for effective feature extraction.

Effect of score mechanism. The quality scoring mechanism evaluates the reliability of trajectory proposals and guides the refinement process. To evaluate its impact, we compare the model with and without this mechanism. The absence of the scoring mechanism results in an increase of 0.0014 in minJointADE, 0.0047 in minJointFDE and CCR slightly increases from 0.1473 to 0.1474. This demonstrates that the quality scoring mechanism effectively enhances the refinement process by prioritizing reliable trajectories.

Effect of different numbers of Mamba layers. We investigate the impact of varying the number of Mamba layers in GAMDTP. Specifically, we test configurations with 1, 3 and 5 layers. The results in Table 3 indicates that more Mamba layers will lead to performance degradation, the minJointADE increases from 0.2529 to 0.2643 in 3 layers and 0.2706 in 5 layers respectively, the minJointFDE increases from 0.8295 to 0.8614 and 0.8687 and the CCR increases

from 0.1474 to 0.1511 and 0.1548, this likely that more layers lead to computational redundancy, resulting in difficulty in convergence. To balance comprehensive performance and computational efficiency, we choose 1 Mamba layer in our GAMDTP network.

5 Conclusion

In this paper, we introduced GAMDTP, a novel framework for accurate and efficient trajectory forecasting in autonomous driving scenarios. By integrating Mamba-SSM and Graph Attention Networks (GAT) through a dynamic gating mechanism, our model effectively captures both local spatial interactions and global temporal dependencies. To further enhance the two-stage trajectory prediction framework, we designed a Quality Scoring Mechanism, which evaluates trajectory proposals and prioritizes high-quality candidates during refinement. Our experimental results on the Argoverse and INTERACTION datasets demonstrate that GAMDTP achieves state-of-the-art performance. In summary, GAMDTP offers a scalable and reliable solution for dynamic trajectory forecasting, advancing the capabilities of autonomous driving systems.

References

1. N. Lee, W. Choi, P. Vernaza, C. B. Choy, P. H. Torr, and M. Chandraker, "Desire: Distant future prediction in dynamic scenes with interacting agents," in *Proceedings of the IEEE conference on computer vision and pattern recognition*, pp. 336–345, 2017.
2. T. Phan-Minh, E. C. Grigore, F. A. Boulton, O. Beijbom, and E. M. Wolff, "Covernet: Multimodal behavior prediction using trajectory sets," in *Proceedings of the IEEE/CVF conference on computer vision and pattern recognition*, pp. 14074–14083, 2020.
3. J. Gao, C. Sun, H. Zhao, Y. Shen, D. Anguelov, C. Li, and C. Schmid, "Vectornet: Encoding hd maps and agent dynamics from vectorized representation," in *Proceedings of the IEEE/CVF conference on computer vision and pattern recognition*, pp. 11525–11533, 2020.
4. M. Liang, B. Yang, R. Hu, Y. Chen, R. Liao, S. Feng, and R. Urtasun, "Learning lane graph representations for motion forecasting," in *Computer Vision—ECCV 2020: 16th European Conference, Glasgow, UK, August 23–28, 2020, Proceedings, Part II 16*, pp. 541–556, Springer, 2020.
5. Y. Wang, S. Zhao, R. Zhang, X. Cheng, and L. Yang, "Multi-vehicle collaborative learning for trajectory prediction with spatio-temporal tensor fusion," *IEEE Transactions on Intelligent Transportation Systems*, vol. 23, no. 1, pp. 236–248, 2020.
6. M. N. Azadani and A. Boukerche, "Stag: A novel interaction-aware path prediction method based on spatio-temporal attention graphs for connected automated vehicles," *Ad Hoc Networks*, vol. 138, p. 103021, 2023.
7. K. Zhang, X. Feng, L. Wu, and Z. He, "Trajectory prediction for autonomous driving using spatial-temporal graph attention transformer," *IEEE Transactions on Intelligent Transportation Systems*, vol. 23, no. 11, pp. 22343–22353, 2022.

8. X. Chen, H. Zhang, F. Zhao, Y. Hu, C. Tan, and J. Yang, "Intention-aware vehicle trajectory prediction based on spatial-temporal dynamic attention network for internet of vehicles," *IEEE Transactions on Intelligent Transportation Systems*, vol. 23, no. 10, pp. 19471–19483, 2022.
9. P. Velickovic, G. Cucurull, A. Casanova, A. Romero, P. Lio, Y. Bengio, *et al.*, "Graph attention networks," *stat*, vol. 1050, no. 20, pp. 10–48550, 2017.
10. S. Hochreiter, "Long short-term memory," *Neural Computation MIT-Press*, 1997.
11. Z. Zhou, L. Ye, J. Wang, K. Wu, and K. Lu, "Hivt: Hierarchical vector transformer for multi-agent motion prediction," in *Proceedings of the IEEE/CVF Conference on Computer Vision and Pattern Recognition*, pp. 8823–8833, 2022.
12. Z. Zhou, J. Wang, Y.-H. Li, and Y.-K. Huang, "Query-centric trajectory prediction," in *Proceedings of the IEEE/CVF Conference on Computer Vision and Pattern Recognition*, pp. 17863–17873, 2023.
13. X. Tang, M. Kan, S. Shan, Z. Ji, J. Bai, and X. Chen, "Hpnet: Dynamic trajectory forecasting with historical prediction attention," in *Proceedings of the IEEE/CVF Conference on Computer Vision and Pattern Recognition*, pp. 15261–15270, 2024.
14. Y. Chai, B. Sapp, M. Bansal, and D. Anguelov, "Multipath: Multiple probabilistic anchor trajectory hypotheses for behavior prediction," *arXiv preprint arXiv:1910.05449*, 2019.
15. J. Gu, C. Sun, and H. Zhao, "Densentnt: End-to-end trajectory prediction from dense goal sets," in *Proceedings of the IEEE/CVF International Conference on Computer Vision*, pp. 15303–15312, 2021.
16. Y. Liu, J. Zhang, L. Fang, Q. Jiang, and B. Zhou, "Multimodal motion prediction with stacked transformers," in *Proceedings of the IEEE/CVF conference on computer vision and pattern recognition*, pp. 7577–7586, 2021.
17. B. Varadarajan, A. Hefny, A. Srivastava, K. S. Refaat, N. Nayakanti, A. Cornman, K. Chen, B. Douillard, C. P. Lam, D. Anguelov, *et al.*, "Multipath++: Efficient information fusion and trajectory aggregation for behavior prediction," in *2022 International Conference on Robotics and Automation (ICRA)*, pp. 7814–7821, IEEE, 2022.
18. A. Vaswani, "Attention is all you need," *Advances in Neural Information Processing Systems*, 2017.
19. A. Gu, K. Goel, and C. Ré, "Efficiently modeling long sequences with structured state spaces," *arXiv preprint arXiv:2111.00396*, 2021.
20. A. Gu and T. Dao, "Mamba: Linear-time sequence modeling with selective state spaces," *arXiv preprint arXiv:2312.00752*, 2023.
21. T. Dao and A. Gu, "Transformers are ssms: Generalized models and efficient algorithms through structured state space duality," *arXiv preprint arXiv:2405.21060*, 2024.
22. O. Lieber, B. Lenz, H. Bata, G. Cohen, J. Osin, I. Dalmedigos, E. Safahi, S. Meirom, Y. Belinkov, S. Shalev-Shwartz, *et al.*, "Jamba: A hybrid transformer-mamba language model," *arXiv preprint arXiv:2403.19887*, 2024.
23. J. Team, B. Lenz, A. Arazi, A. Bergman, A. Manevich, B. Peleg, B. Aviram, C. Almagor, C. Fridman, D. Padnos, *et al.*, "Jamba-1.5: Hybrid transformer-mamba models at scale," *arXiv preprint arXiv:2408.12570*, 2024.
24. W. He, K. Han, Y. Tang, C. Wang, Y. Yang, T. Guo, and Y. Wang, "Densemamba: State space models with dense hidden connection for efficient large language models," *arXiv preprint arXiv:2403.00818*, 2024.
25. L. Zhu, B. Liao, Q. Zhang, X. Wang, W. Liu, and X. Wang, "Vision mamba: Efficient visual representation learning with bidirectional state space model," *arXiv preprint arXiv:2401.09417*, 2024.

26. K. Li, X. Li, Y. Wang, Y. He, Y. Wang, L. Wang, and Y. Qiao, "Videomamba: State space model for efficient video understanding," in *European Conference on Computer Vision*, pp. 237–255, Springer, 2025.
27. Z. Zhang, A. Liu, I. Reid, R. Hartley, B. Zhuang, and H. Tang, "Motion mamba: Efficient and long sequence motion generation," in *European Conference on Computer Vision*, pp. 265–282, Springer, 2025.
28. R. Ding, K.-D. Luong, E. Rodriguez, A. C. A. L. da Silva, and W. Hsu, "Combining graph neural network and mamba to capture local and global tissue spatial relationships in whole slide images," *arXiv preprint arXiv:2406.04377*, 2024.
29. Y. Zhou, H. Shao, L. Wang, S. L. Waslander, H. Li, and Y. Liu, "Smartrefine: A scenario-adaptive refinement framework for efficient motion prediction," in *Proceedings of the IEEE/CVF Conference on Computer Vision and Pattern Recognition*, pp. 15281–15290, 2024.
30. M.-F. Chang, J. Lambert, P. Sangkloy, J. Singh, S. Bak, A. Hartnett, D. Wang, P. Carr, S. Lucey, D. Ramanan, *et al.*, "Argoverse: 3d tracking and forecasting with rich maps," in *Proceedings of the IEEE/CVF conference on computer vision and pattern recognition*, pp. 8748–8757, 2019.
31. W. Zhan, L. Sun, D. Wang, H. Shi, A. Clausse, M. Naumann, J. Kummerle, H. Konigshof, C. Stiller, A. de La Fortelle, *et al.*, "Interaction dataset: An international, adversarial and cooperative motion dataset in interactive driving scenarios with semantic maps," *arXiv preprint arXiv:1910.03088*, 2019.
32. R. M. Schmidt, "Recurrent neural networks (rnns): A gentle introduction and overview," *arXiv preprint arXiv:1912.05911*, 2019.
33. A. Zyner, S. Worrall, and E. Nebot, "Naturalistic driver intention and path prediction using recurrent neural networks," *IEEE transactions on intelligent transportation systems*, vol. 21, no. 4, pp. 1584–1594, 2019.
34. Y. Xing, C. Lv, and D. Cao, "Personalized vehicle trajectory prediction based on joint time-series modeling for connected vehicles," *IEEE Transactions on Vehicular Technology*, vol. 69, no. 2, pp. 1341–1352, 2019.
35. A. Alahi, K. Goel, V. Ramanathan, A. Robicquet, L. Fei-Fei, and S. Savarese, "Social lstm: Human trajectory prediction in crowded spaces," in *Proceedings of the IEEE conference on computer vision and pattern recognition*, pp. 961–971, 2016.
36. N. Deo and M. M. Trivedi, "Convolutional social pooling for vehicle trajectory prediction," in *Proceedings of the IEEE conference on computer vision and pattern recognition workshops*, pp. 1468–1476, 2018.
37. L. Hou, S. E. Li, B. Yang, Z. Wang, and K. Nakano, "Structural transformer improves speed-accuracy trade-off in interactive trajectory prediction of multiple surrounding vehicles," *IEEE Transactions on Intelligent Transportation Systems*, vol. 23, no. 12, pp. 24778–24790, 2022.
38. Z. Li, Y. Wang, and Z. Zuo, "Interaction-aware prediction for cut-in trajectories with limited observable neighboring vehicles," *IEEE Transactions on Intelligent Vehicles*, vol. 8, no. 3, pp. 2148–2161, 2023.
39. J. Ngiam, B. Caine, V. Vasudevan, Z. Zhang, H.-T. L. Chiang, J. Ling, R. Roelofs, A. Bewley, C. Liu, A. Venugopal, *et al.*, "Scene transformer: A unified architecture for predicting multiple agent trajectories," *arXiv preprint arXiv:2106.08417*, 2021.
40. D. Wang, K. Tang, J. Zeng, Y. Pan, Y. Dai, H. Li, and B. Han, "Mm-transformer: A transformer-based knowledge graph link prediction model that fuses multimodal features," *Symmetry*, vol. 16, no. 8, p. 961, 2024.
41. N. Carion, F. Massa, G. Synnaeve, N. Usunier, A. Kirillov, and S. Zagoruyko, "End-to-end object detection with transformers," in *European conference on computer vision*, pp. 213–229, Springer, 2020.

42. S. Ren, K. He, R. Girshick, and J. Sun, "Faster r-cnn: Towards real-time object detection with region proposal networks," *IEEE transactions on pattern analysis and machine intelligence*, vol. 39, no. 6, pp. 1137–1149, 2016.
43. T. Gilles, S. Sabatini, D. Tsishkou, B. Stanciulescu, and F. Moutarde, "Thomas: Trajectory heatmap output with learned multi-agent sampling," *arXiv preprint arXiv:2110.06607*, 2021.
44. T. Gilles, S. Sabatini, D. Tsishkou, B. Stanciulescu, and F. Moutarde, "Home: Heatmap output for future motion estimation," in *2021 IEEE International Intelligent Transportation Systems Conference (ITSC)*, pp. 500–507, IEEE, 2021.
45. Z. Huang, X. Mo, and C. Lv, "Multi-modal motion prediction with transformer-based neural network for autonomous driving," in *2022 International Conference on Robotics and Automation (ICRA)*, pp. 2605–2611, IEEE, 2022.
46. H. Chen, J. Wang, K. Shao, F. Liu, J. Hao, C. Guan, G. Chen, and P.-A. Heng, "Traj-mae: Masked autoencoders for trajectory prediction," in *Proceedings of the IEEE/CVF International Conference on Computer Vision*, pp. 8351–8362, 2023.
47. X. Jia, P. Wu, L. Chen, Y. Liu, H. Li, and J. Yan, "Hdgt: Heterogeneous driving graph transformer for multi-agent trajectory prediction via scene encoding," *IEEE transactions on pattern analysis and machine intelligence*, 2023.
48. L. Rowe, M. Ethier, E.-H. Dykhne, and K. Czarnecki, "Fjmp: Factorized joint multi-agent motion prediction over learned directed acyclic interaction graphs," in *Proceedings of the IEEE/CVF Conference on Computer Vision and Pattern Recognition*, pp. 13745–13755, 2023.